REPORT DOCUMENTATION PAGE

Form Approved
OMB No. 0704-0188

1. AGENCY USE ONLY (*Leave Blank*)	2. REPORT DATE	3. REPORT TYPE AND DATES COVERED
	30 July 1997	Final, 3/13/96 - 6/27/97

4. TITLE AND SUBTITLE

Passive Shielding for Low Frequency Magnetic Films

5. FUNDING NUMBERS

DAAE30-96-C-0022

6. AUTHOR(S)

Dr. Nickander J. Damaskos
Dr. Benuel J. Kelsall
Mr. Mark A. Smoot

7. PERFORMING ORGANIZATION NAME(S) AND ADDRESS(ES)

Damaskos, Inc.
P.O. Box 469
Concordville, PA 19331

8. PERFORMING ORGANIZATION REPORT NUMBER

C0329-1

9. SPONSORING/MONITORING AGENCY NAME(S) AND ADDRESS(ES)

US Army TACOM-ARDEC
AMSTA-AR-PC-G, Bldg 9
Picatinny Arsenal, NJ 07806

10. SPONSORING/MONITORING AGENCY REPORT NUMBER

11. SUPPLEMENTARY NOTES

12a. DISTRIBUTION/AVAILABILITY STATEMENT

Approved for public release; distribution unlimited

12b. DISTRIBUTION CODE

13. ABSTRACT (*Maximum 200 words*)

Report developed under SBIR Contract. An approach to low frequency shielding is shown with application to suppression of electromagnetic fields emanating from rail gun barrels and power cable busses. Damaskos, Inc.'s Thin-Shield™ materials are applied to a scaled electric gun barrel as continuous unbroken coatings that are directly deposited onto the barrel and as planar coatings that are wrapped around the barrel. Significant attenuations are observed in both cases. Shielding effectiveness of the order of 30 dB was measured from 10 Hz to 1000 Hz and above. An analysis in cylindrical coordinates confirms the qualitative behavior of observed near field shielding effectiveness for non-magnetic coating. Further refinement of the numerical computation is required to model a magnetic coating. Recommendations are offered for further development and scaled up demonstrations.

14. SUBJECT TERMS			15. NUMBER OF PAGES
SBIR Report	Shielding Magnetic	Near Field Low Frequency	43 16. PRICE CODE

17. SECURITY CLASSIFICATION OF REPORT	18. SECURITY CLASSIFICATION OF THIS PAGE	19. SECURITY CLASSIFICATION OF ABSTRACT	20. LIMITATION OF ABSTRACT
UNCLASSIFIED	UNCLASSIFIED	UNCLASSIFIED	

PASSIVE SHIELDING FOR LOW FREQUENCY MAGNETIC FIELDS

FINAL REPORT

July 30, 1997

for

US Army Armament R, D & E Center
Code: AMSTA-AR-CCL-D/Mr. K. O'Malley
Picatinny Arsenal, NJ 07806-5000

under

Contract DAAE30-96-C-0022

by

Damaskos, Inc.
P. O. Box 469
Concordville, PA 19331
(610) 358-0200
FAX (610) 558-1019

ABSTRACT

An approach to low frequency shielding is shown with application to suppression of electromagnetic fields emanating from rail gun barrels and power cable busses. Damaskos, Inc.'s Thin-Shield™ materials are applied to a scaled electric gun barrel as continuous unbroken coatings that are directly deposited onto the barrel and as planar coatings that are wrapped around the barrel. Significant attenuations are observed in both cases. Shielding effectiveness of the order of 30 dB was measured from 10 Hz to 1000 Hz and above. An analysis in cylindrical coordinates confirms the qualitative behavior of observed near field shielding effectiveness for non-magnetic coating. Further refinement of the numerical computation is required to model a magnetic coating. Recommendations are offered for further development and scaled up demonstrations.

TABLE OF CONTENTS

Page

Title Page i

Abstract ii

Table of Contents iii

Background 1

Statement of the Problem and Goals 1

Technical Approach 1

Fabrication of the Shielding Materials 3

Approach 3

Plating by Direct Deposition 3

Plating onto Planar Wrappable Sheets 6

Electroplating Process 9

Plating Density 9

Scale Up of direct Plating Process 9

Other Applications of the Shielding Process 10

Analysis 11

Experimental Setup and Measurements 12

Measured Results 14

Direct Deposition Gun Barrels 14

Wrapped Gun Barrels 19

Measurements Summary 24

Discussion of Results 24

Calculations 25

Calculations Summary 30

Conclusions and Recommendations 31

Recommendations 32

References 34

Appendix A - Cylindrical Wave Electric Field Shielding Analysis 35

Appendix B - Cylindrical Wave Magnetic Field Shielding Analysis 38

BACKGROUND

Statement of the Problem and Goals

The main objective of this Phase I effort is to demonstrate a coating for shielding the near field magnetic fields in two applications, the electric rail gun and electric power busses. Both geometries are of a cylindrical nature and are studied using high aspect ratio cylinders in the presence of an applied magnetic field. The goal is to show significant low frequency attenuation from about 10 Hz to 1 kHz and beyond, and a practical means for achieving the attenuation. Levels of 30 dB or more are sought and the type of coating is to be defined.

Because of the demonstrated success of Damaskos, Inc.'s multilayered ThinShield™ coatings from about 100 kHz through the microwave bands, basic ThinShield™ materials are suggested and explored at this lower portion of the spectrum. The cited band not only embraces the frequencies associated with firing a rail gun, but also includes 60 Hz and the tens of harmonics of 60 Hz produced during generation of electric power. ThinShield™ materials consist of layers of high permeability alternating with layers of high conductivity. The figure of merit of the materials is the $\mu\sigma$ product (where μ is permeability and σ is bulk conductivity). In particular nickel alloy and copper are the materials of effective ThinShield™ coatings and are used here.

Technical Approach

The main technical consideration is the physical scale of the feasibility demonstration. The scale is dictated by the present limitations on the size of objects that can be coated and limitations on the size of the wrappable sheets. To satisfy the concept, Phase I addresses the direct deposition of a nickel alloy coating onto a thin cylindrical metal tube which then forms a one layer pair ThinShield™ structure around the scaled gun barrel. In this manner, the effects of breaks in the coating that are found in the more practicable wrappable shielding structure, do not manifest themselves. Thus direct deposit provides a more ideal structure that can be studied with suitable analysis and also a practical performance limit (goal) when dealing with the break or gap issue. The physical size of the simulated gun barrel tubes in a nominal 10 1/2" length by 3/4" diameter by 1/32" thick copper tube. Besides these plating and coating considerations, the large Helmholz coil apparatus that generates the applied magnetic field limits the size of the scaled tube to its sweet or uniform spot of roughly 12".

Several tubes of equal length were cut and one served as a control or reference against which all ThinShield™ pair coatings were compared. The shielding performance measure is the ratio of the magnetic field intensity at the center of the Helmholz coil setup with and without the reference scale gun barrel and with and without the ThinShield™ coated scaled gun. The latter ratio divided by the reference tube ratio defines the shielding effectiveness whose square is expressed in decibels as a function of frequency.

Certain additional practical constraints are imposed on the demonstration such as: available output power in the low frequency band of interest; sensitive detection of the shielded magnetic fields; having to deal with the nonlinear form (due to saturation) of the detected fields because of the limited dynamic range of the measurements; and others.

Analysis is considered important to the definition and development of a coating. The main point here is to have available a cylindrical coordinate multilayer model in which the near field magnetic fields inside and external to a shield can be calculated as a function of frequency and the shield materials' constitutive parameters. In so far as the model is predictive it can serve as a design and optimization tool. A draw back to many models concerns their inherent high impedance (i.e. E-field) wave formulation wherein the essence of the low frequency near field magnetic character is not physically incorporated. Planar one-dimensional and cylindrical models were exercised.

And, there is the new technical area of direct deposition of ThinShield™ coatings following Damaskos, Inc. experience with planar wrappable sheet depositions. New setups were required here.

These factors and others define the technical approach that was followed. The results are reported below as are further aspects and recommendations for work that would continue into a Phase II effort.

FABRICATION OF THE SHIELDING MATERIALS

Approach

A ferrous-nickel alloy is proposed for use as the magnetic component of a ThinShield™ composite structure to provide local passive attenuation of the intense low frequency magnetic fields associated with the operation of an electromagnetic projectile launcher referred to as a rail gun. Copper is the non-magnetic component of the composite structure. The over-all functional shape of this shielding application has a cylindrical geometry that either wraps or otherwise encloses the electric barrel portion of the launcher. Two forms of shield were produced and each of these approaches to enclosure configuration were investigated and evaluated.

Plating by Direct Deposition

The first shielding material produced is a continuous-concentric cylindrical design, electroplated on the outside diameter of a series of prepared copper tubes. These tubes are ~10 1/2 inch long and were cut from a length of high purity, oxygen free (HPOF) copper stock having an 0.032 inch wall thickness and a 3/4 inch outside diameter. They were mechanically smoothed and chemically cleaned in preparation for plating and then weighed to the nearest gram. The nominal mass of each is ~110 grams.

In this process the copper tube serves as the plating substrate and cathode electrode. The ends of each tube are inserted in terminal fitting connectors wired to the negative output of a direct current (DC) power supply. The copper tube-cathode assembly is centered inside a nickel alloy tube. A circular band was fashioned as an electrical connector fitting and fixed to the outside diameter of the nickel tube. The positive output of the DC power supply was wired to this band so that the nickel tube functions as the anode during the electroplating process. See Figure 1.

During the course of the electroplating process the shielding alloy grows or plates onto the copper-cathode tube over its nominal 9 inch (exposed) length, providing an effective surface area of ~21.20 in^2 or ~0.147 ft^2 exposure to the plating bath. At the conclusion of each electroplating run, the tube is removed from the bath fixturing, rinsed with tap water, thoroughly dried and weighed to the nearest gram. This process yielded tubes having a

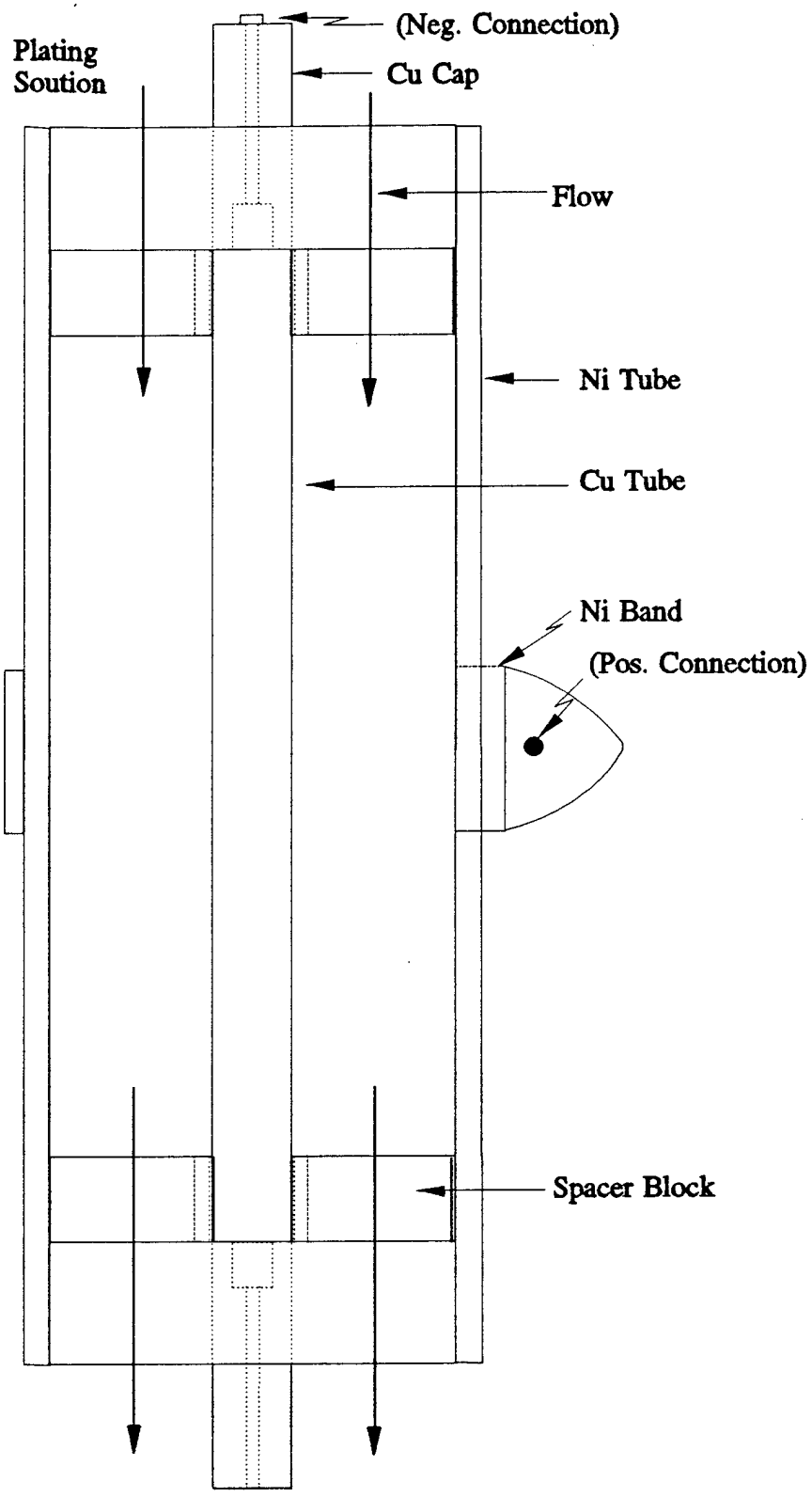

Figure 1. Cross section of copper tube-cathode assembly inserted into nickel anode fixture used to produce the continuous, cylindrical geometry shielding material.

Table 1. Physical measurement data of the magnetic shielding alloy electroplated on copper tube substrates in the continuous-concentric cylindrical geometry.

	Copper Tubes		
	1	2	3
Electroplating time (hr)	3	5.5	8
Current density (A/ft^2)	23.1	21.1	27.2
Mass gain (g)	11	18	36
Mass growth rate (g/hr)	3.7	3.3	4.5
Average radius increase (cm)	0.010	0.016	0.032
Average plating thickness (mils)	3.9	6.6	12.5
Thickness growth rate (mil/hr)	1.2	1.2	1.6
Volume of plated material (cm^3)	1.37	2.23	4.37
Average alloy density obtained from dimensional and mass changes (g/cm3)	~8.0	8.1	8.1

bright lustrous, continuous alloy coating, to a depth principally determined by the time and current density parameters. See Table 1. Shielding measurements are then made on these tubes.

Plating onto Planar Wrappable Sheets

The second shielding design is fabricated in a bilateral planar geometry by plating the nickel alloy onto a copper foil substrate of ~0.7 mils thickness and nominal dimensions of ~14 1/4 inch by ~14 3/4 inch. The total area exposed to the plating solutions is ~420 in^2 or ~2.92 ft^2. A chemical system is used to clean and prepare the foil for the plating process. A mounting frame was constructed from HPOF copper bars and plastic rod, that mechanically supports and tensions the copper foil while it is immersed in the tank bath during the electroplating process. The frame also functions as the cathode terminal fitting through its continuous electrical contact along the two vertical edges of the suspended foil. Two nickel alloy plates are inserted into accommodations in this same bath fixture, where they are secured directly on either side of the foil frame-cathode assembly. Electrical connections are made to these two plates that are in turn wired to the positive output of the DC power supply, causing them to function as anodes when a current is applied to the A-C circuit during the course of the plating process.

Figure 2 shows the mounting of the copper and nickel anode assembly. At the conclusion of each bilateral planar electroplating run, the foil frame-cathode assembly is removed from the bath and rinsed with tap water. The sheet of smooth, bright alloy shielding material is released from the support frame, thoroughly dried and weighed to the nearest gram. See Table 2. It is then rolled into a cylindrical shape in preparation for the shielding measurements, by forming a tube configured with multiple contiguous, spiral wraps.

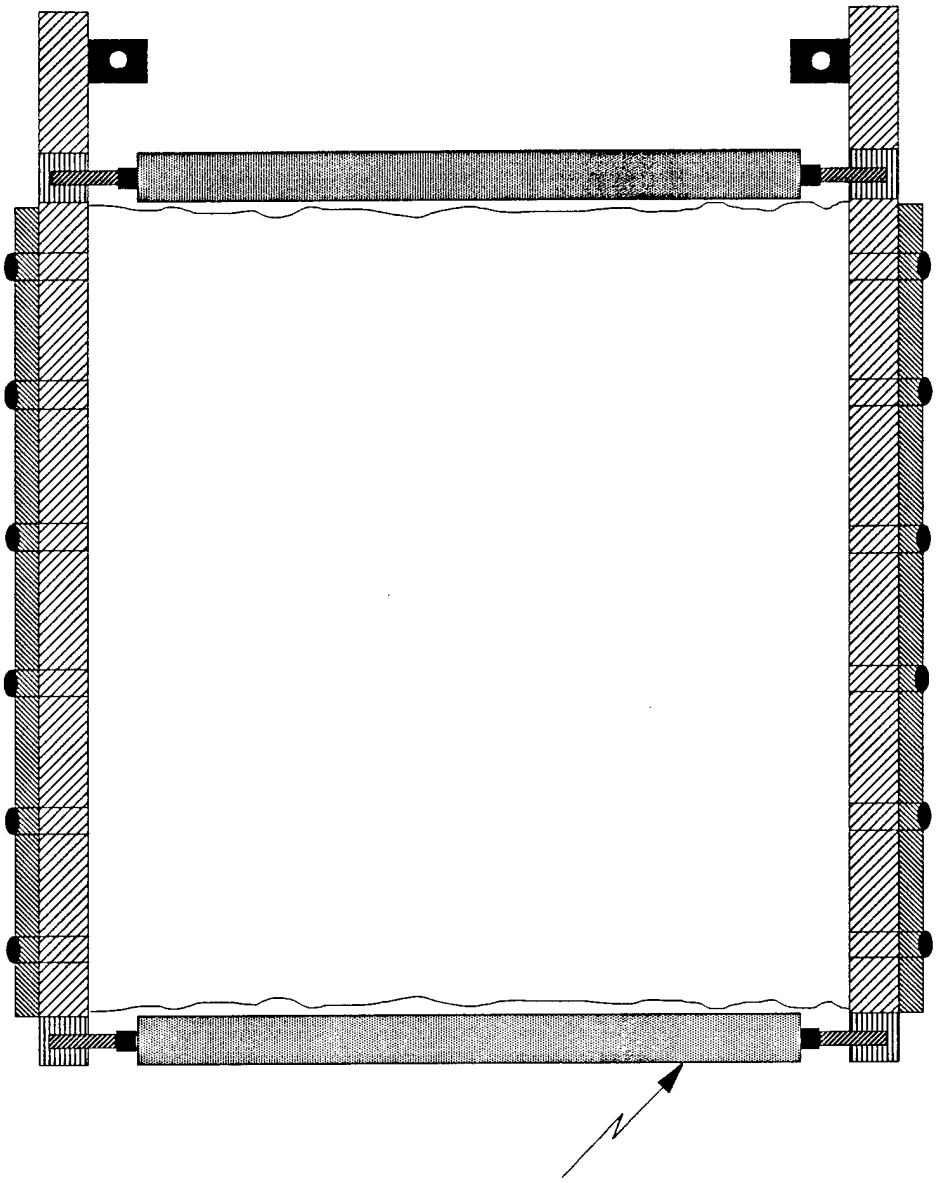

Figure 2. Drawing of the copper foil support frame-cathode fixture used to produce the bilateral planar geometry shielding material.

Table 2. Physical measurement data from the magnetic shielding alloy material electroplated on copper foil substrates in the bilateral planar geometry.

	Copper Foil Substrates						
	1	2	3	4	5	6	7
Electroplating times (hr)	1	1/2	3	1	2	1/2	3
Current Density (A/ft2)	17.1	8.6	17.1	17.1	17.1	17.1	17.1
Mass Gain (g)	46	11	130	47	85	23	138
Mass Growth Rate (g/hr)	46	44[1]	43.3	47	42.5	44[1]	46
Average Plating Thickness (mils)	1.4	0.34	4.4	1.6	3.3	0.8	4.6
Thickness Growth Rate (mil/hr)	1.4	1.2[1]	1.5	1.6	1.7	1.6[1]	1.5
Average Volume of Plated Material (cm^3)	5.42	1.28	15.19	15.56	10.20	2.71	15.87
Average Alloy Density obtained from dimensional and mass changes (g/cm^3)	8.5	8.6	8.6	8.5	8.3	8.5	8.6

1. Values extrapolated to an hour basis.

Electroplating Process

The plating bath is an aqueous based solution consisting of nickel sulfate, nickel chloride, boric acid, ferrous sulfate and wetting agent. The wetting agent was added to the plating bath to lower the surface tension of the aqueous solution. Additionally the wetting agent helps minimize the residual tensile stress incorporated in the plated material. These constituents were systematically added to distilled water in the plating tank, heated, mixed and filtered.

Initially shielding material was deposited on a prepped copper tube loaded into the nickel cylinder fixture to determine the parameters that provided good plating quality. A bath temperature of 68-76°C, pH of ≈ 3.1, and current density of 17-27 A/ft^2 were determined.

Plating Density

The measurement data from both fabrication approaches are displayed in a later section. A speculative working number of 8.20 g/cm^3 was proposed as a figure of merit for a density, to gauge the first series of plating deposits. The obtained values of 8.0 to 8.1 g/cm^3 for the cylindrical plating geometry were considered to be in good agreement with the assumed value, based on the accuracy limit of the measurement method. Owing to the absence of any noted parameter change, the range of densities obtained in the bilateral planar plating geometry represent the formidable challenge of accurately measuring the true alloy sheet thickness, rather than reflecting a shift in nickel alloy composition. The sheets of plated alloy measured $\sim 20\%$ thicker along the two horizontal edges not in contact with the electrodes. This may be due to some local field influence by the copper bar electrode, securing the copper foil substrate.

Scaleup of Direct Plating Process

From a scaling-up perspective using fixed dimension copper tubes or copper coated tubes as cathode-substrate structures, the basic approach developed in the process appears to be well suited for producing shielding alloy on as large a cylinder as desired. There may exist a size limitation with respect to changes in current/voltage characteristics along an

extended length of cathode tubing, impacting on growth rates and causing thickness variations in the plating. If longer/larger tube substrates are desired, a horizontal bath fixture orientation might be helpful in reducing temperature stratification in the bath, adversely affecting the uniformity of the plating quality. With respect to throughput or production rate, this approach may lend itself more readily to a batch production mode rather than a continuous in-line plating process. The shielding alloy plated on the copper foil substrate demonstrated good ductility and adhesion characteristics throughout all plating thicknesses and wrapping configurations. A larger scale production of shielding alloy using a film or foil substrate may be more efficiently accomplished through an in-line, continuous feed electroplating process, rather that a batch method.

Other Applications of the shielding Process

Some additional applications for this type of shielding material range from consumer products such as, appliances like electric hair driers, having relatively high fields associated with their operation, to portable electronic equipment such as cellular telephone, computers, and radio transceivers. Implanted medical devices such as cardiac pacemakers, as well as portions of myriad electronic instruments/equipment sensitive to extraneous EMI/RFI signals, may benefit from an enclosure of this shielding material. Testing cells or complete rooms could be made relatively impervious to incoming or outgoing EMI/RFI signals within the frequency band and attenuation range of this material.

ANALYSIS

Calculations were made with three analyses. The first is Damaskos, Inc.'s own proprietary code TROMMA; the second is the analysis that was included in the Phase I proposal (and is presented as Appendix A); the third is a new analysis. The first two analyses concern multilayered ThinShield™ coatings in planar (TROMMA) and cylindrical (second analysis) geometries for E-field excitation where the wave impedances are 377Ω. The results of these efforts are described in later text. Suffice it to say that a cylindrical analysis for magnetic (H-field) field excitation in the near field was required and an analysis of a single tubular material carrying a current was made and is presented in Appendix B.

EXPERIMENTAL SETUP AND MEASUREMENTS

The setup for the measurements consists of a Helmholtz coil to generate a time varying magnetic field and a small pickup coil to measure the strength of the magnetic field. Since the shielding properties were desired, relative measurements were made instead of absolute measurements. The relative measurements were made by taking the ratio of field inside the simulated gun barrel and the field strength in the absence of the barrel.

The Helmholtz coils are driven with a high current Kepco power supply. The frequency was set by a Hewlett-Packard function generator that can produce a sinusoidal wave form from less than 10 Hz to more than 4000 Hz. The current passing through the Helmholtz coils is monitored by the voltage drop across a 1 ohm resistor in series with the coils. An oscilloscope is used to monitor the voltage and display the waveform and to verify the frequency of the current.

A small coil is used to detect fields. A piece of coaxial cable is used to connect the coil with the oscilloscope. The coax is used to prevent the system from responding to stray fields. (An earlier version using a pair of twisted wires did exhibit interference from stray fields.) The coax also serves to support the coil and hold it in the proper orientation. The oscilloscope allows for the measurement of the voltage across the coil as well as showing the waveform.

Figure 3 shows a schematic of the setup.

Table 3 shows the magnetic field strength calculated for the center of the Helmholtz coils for the different measurement frequencies. This is determined from the number of turns used in the coils, the geometry of the coils, and the current that passes through the coils.

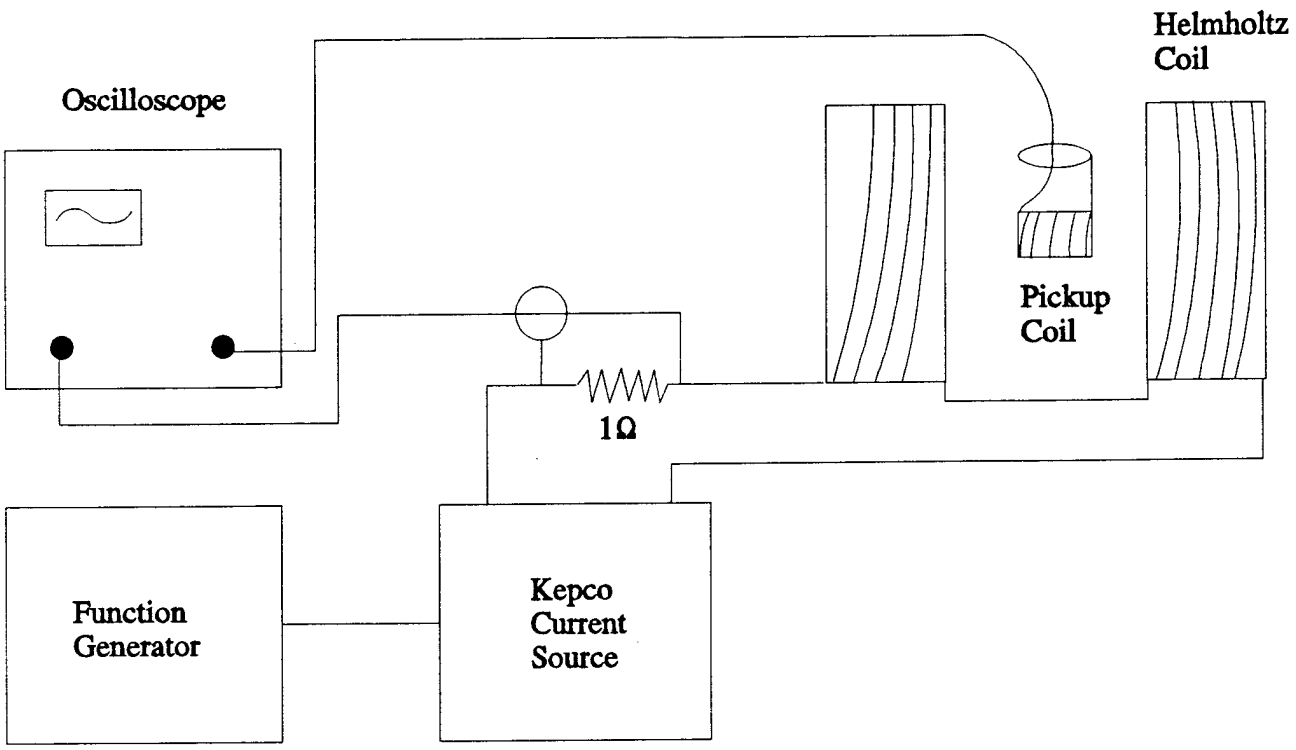

Figure 3. Schematic of setup showing key components.

Table 3. Field strength in center of Helmholtz coils.

Freq (Hz)	H (Amp/m)	Gauss
10	1477	18.6
20	779	9.8
40	352	4.4
80	182	2.3
100	148	1.9
200	83	1.0
400	35	0.43
800	18	0.22
1000	14	0.18
2000	6	0.08
4000	0.8	0.01

Measured Results

Direct Deposit Gun Barrels.

Six simulated rail gun barrels were prepared; three had a nickel alloy electrodeposited on them, one had two turns of a thin nickel alloy sheet wrapped around it, one had copper electrodeposited on it, and the last one was left bare and was used as a reference for all measurements. Table 4 lists the results of the measurements. The listing gives the measurement of the field inside the tube vs the field when the simulated gun barrel is not present. This quantity is expressed as a transmission coefficient in dB. These data are also plotted in Figures 4 to 6.

The table shows that for low frequency measurements some distortion was observed for all alloy samples. To explore this phenomenon, 20, 40, and 80 Hz were selected and the driving current to the Helmholtz coils was reduced. When the power was reduced the waveform detected by the pick up coil in the simulated gun barrel changed shape, but it did not become sinusoidal before the signal was lost in the noise due to lack of sensitivity.

Figure 4. Nickel Alloy Direct Deposit on Model Rail Gun

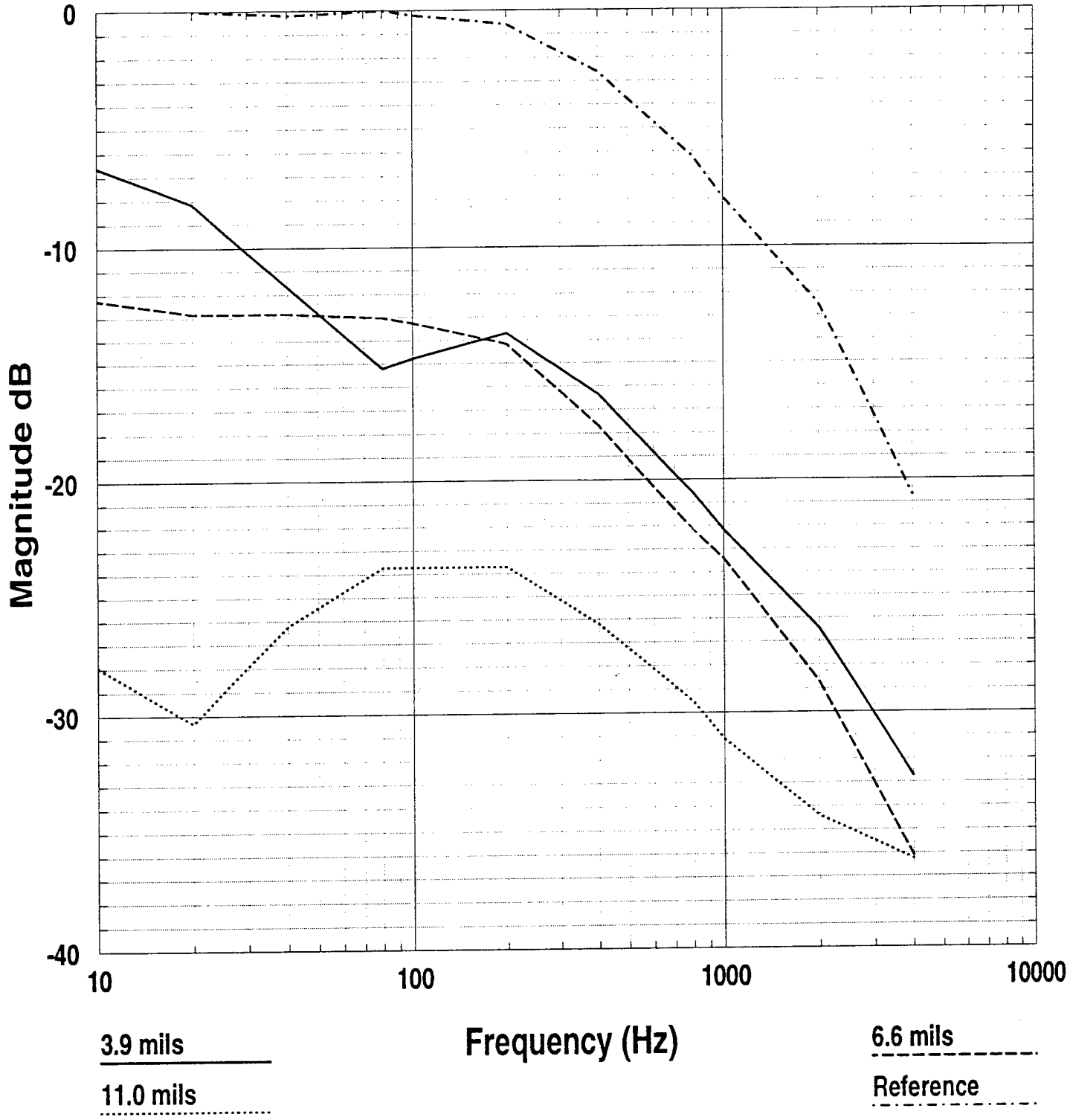

Figure 5. Copper Deposit on Copper Tube

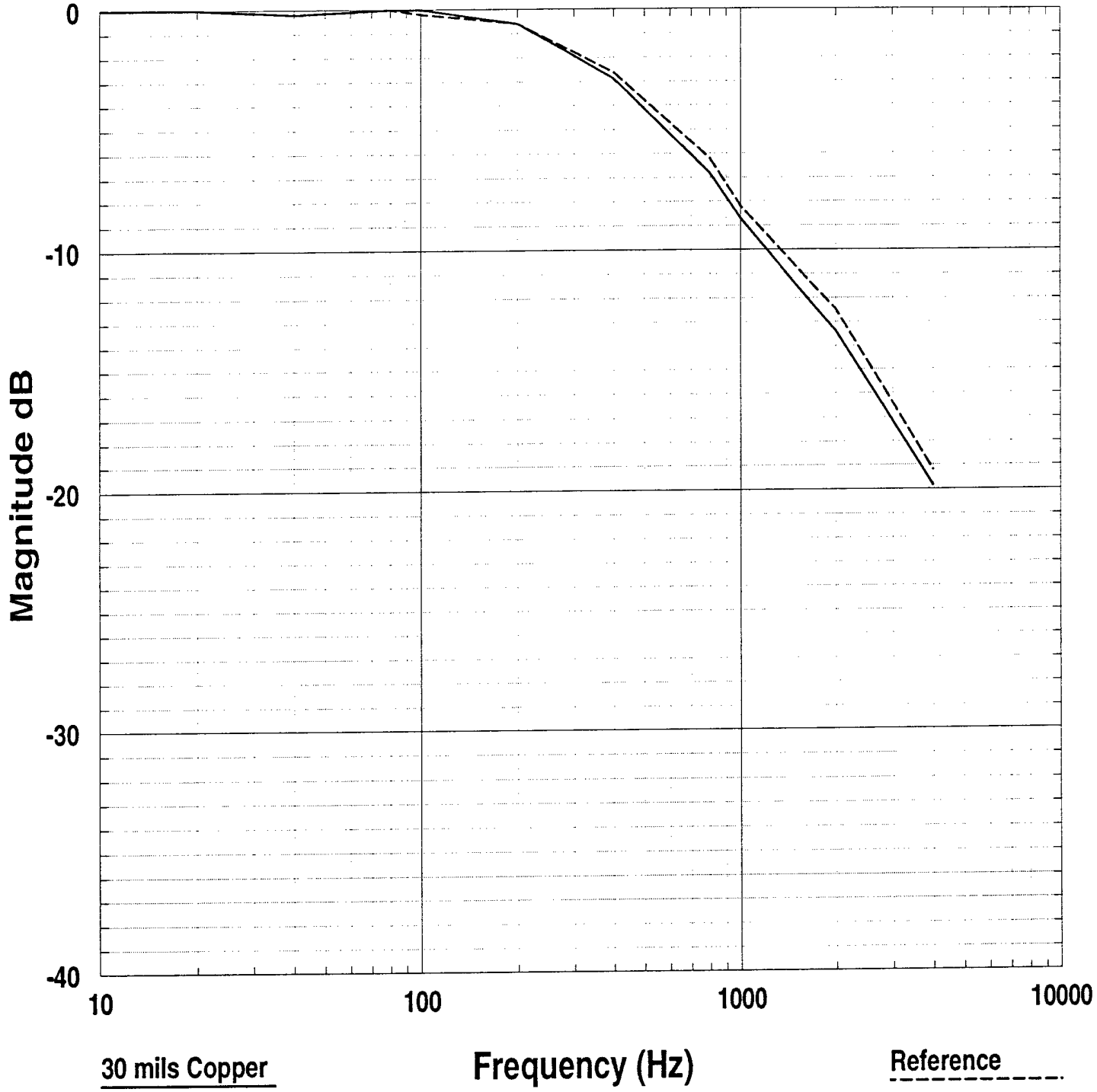

Figure 6. Thin Nickel Alloy Sheet Wrap on Copper Tube

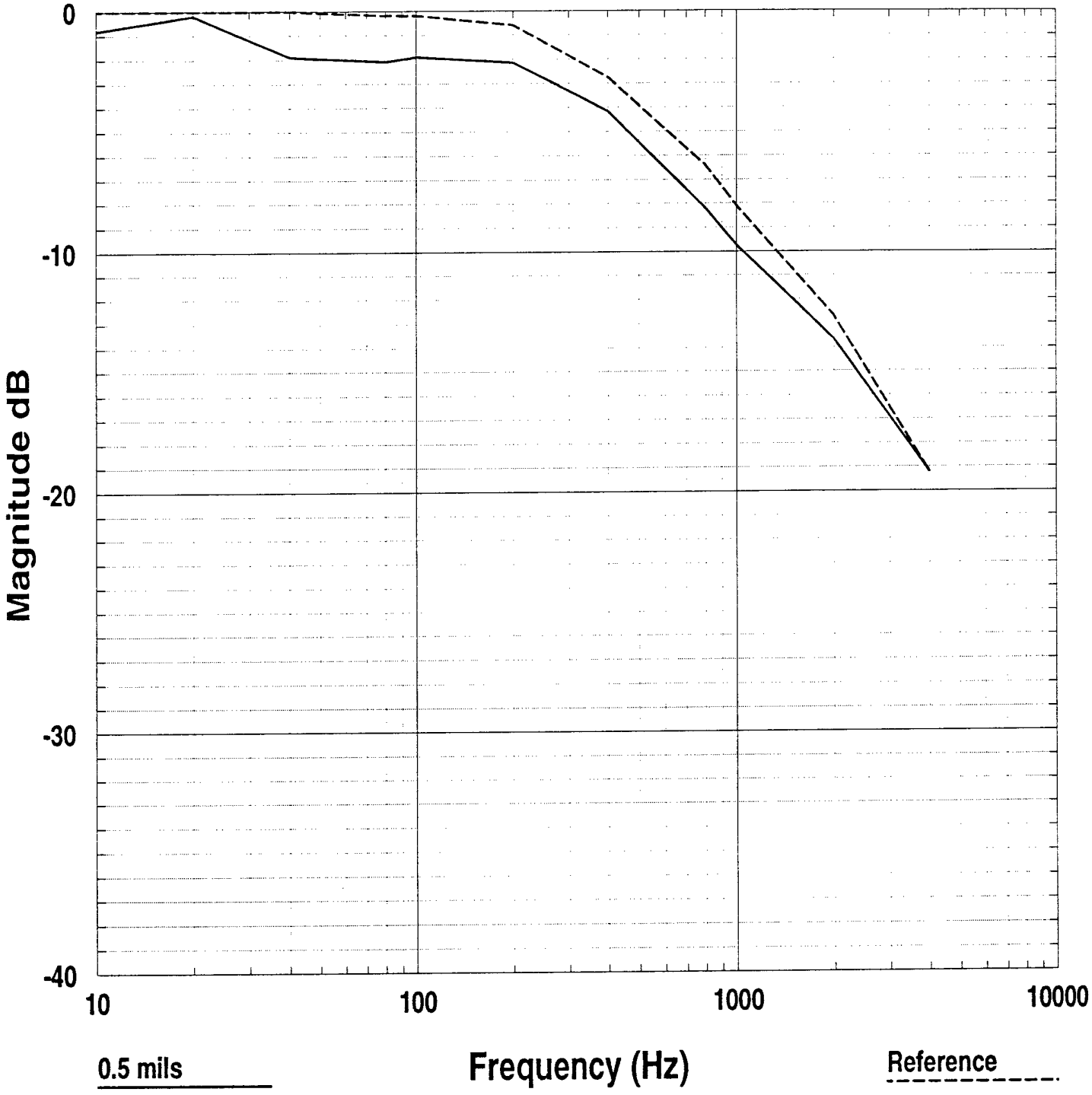

Table 4. Measured transmission coefficients (dB relative to free space) for direct deposit on gun barrel.

Freq (Hz)	Copper		Nickel Alloy			
	Bare	30 Mils	11 mils	6.6 mils	3.9 mils	Thin Sheet 0.5 mils
10	0.0	0.0	-28.0*	-12.2*	-6.6*	-0.8*
20	0.0	0.0	-30.3*	-12.8	-8.1*	-0.2*
40	0.0	-0.2	-26.2*	-12.8	-11.7*	-1.9*
80	0.0	0.0	-23.7	-13.0	-15.2*	-2.1
100	-0.2	0.0	-23.7	-13.3	-14.8	-1.9
200	-0.6	-0.6	-23.7	-14.2	-13.7	-2.1
400	-2.6	-2.9	-26.2	-17.7	-16.4	-4.2
800	-6.2	-6.8	-29.5	-22.2	-20.6	-8.2
1000	-7.7	-8.7	-31.1	-23.4	-22.2	-9.7
2000	-12.5	-13.4	-34.4	-28.7	-26.4	-13.7
4000	-20.6	-19.9	-36.3	-36.1	-32.7	-19.2

* Indicates that the waveform is distorted.

As part of this study, the wave form was examined as the simulated gun barrel was slipped over the pickup coil. Maximum shielding is reached once the probe is about 1 to 2 inches (depends on the deposit) inside the coated region. Further insertion into the coated region does not alter the level of shielding, but the waveform changes shape in random ways. It was also observed that the waveform shape could be altered by rotating the tube about its long axis.

A summary of the average magnetic shielding performance is given in Table 5 and was obtained from a direct column average of the entries in Table 4. Note that the copper deposit only increases the shielding by a very small amount. The attenuation of the magnetic field by the presence of the nickel alloy is proportional to the amount of alloy deposited. Although the data do not show a perfect correlation, this may be due to the deposition bath changing characteristics with time and it may be due to the inability to measure the thickness.

Table 5. Comparison of average transmission coefficient (10 to 4000 Hz) and average transmission coefficient of nickel alloy coating per unit thickness.

Bare	11.0 mils	6.6 mils	3.9 mils	30 mils Cu	Thin Sheet 0.5 mils
-4.58 dB	-28.46 dB	-18.76 dB	-17.13 dB	-4.77 dB	-5.82 dB
Not Applicable	-2.17 dB/mil	-2.15 dB/mil	-3.22 dB/mil	-0.01 dB/mil	-2.48 dB/mil

The last row in Table 5 is the average shielding per mil of coating. This number is obtained by first subtracting the contribution due to the copper tube and then dividing by the thickness of the deposit. These numbers show that the shielding efficiency of the nickel alloy decreases as the thickness of the deposit increases even though the total shielding increases. Note also that the shielding effectiveness per unit thickness of the thin 0.5 mil sheet is not as good as the direct deposit effectiveness. This may be due to the wrap technique as opposed to the quality of the material.

Wrapped Gun Barrels

Seven runs were made where nickel alloy was electro-deposited on both sides of 0.7 mil copper foil. The foil was then wrapped into a small tube of approximately the same size as the copper tubes. Since the foil tubes are very rigid, the copper tube used as a form was removed before measurements. In some cases, the foil was too stiff to wrap into a small tube using reasonable means; as a result the diameter and number of turns for some of the tubes vary.

Table 6 summarizes the data. The table shows the number of turns and the thickness of the nickel alloy for each run. Note that alloy is deposited on both sides of the 0.7 mil foil and that the number reported in the table is the combined thickness on both sides. Note further that the thickness of the deposition varies across the sheet and that the thickness is greater at the edges. The thickness reported in the table is based on the mass pickup for the entire sheet. The data listed in Table 6 are plotted in Figures 7 and 8. Figure 7 shows that

Figure 7. Nickel Alloy Coatings on Copper Foil Wraps

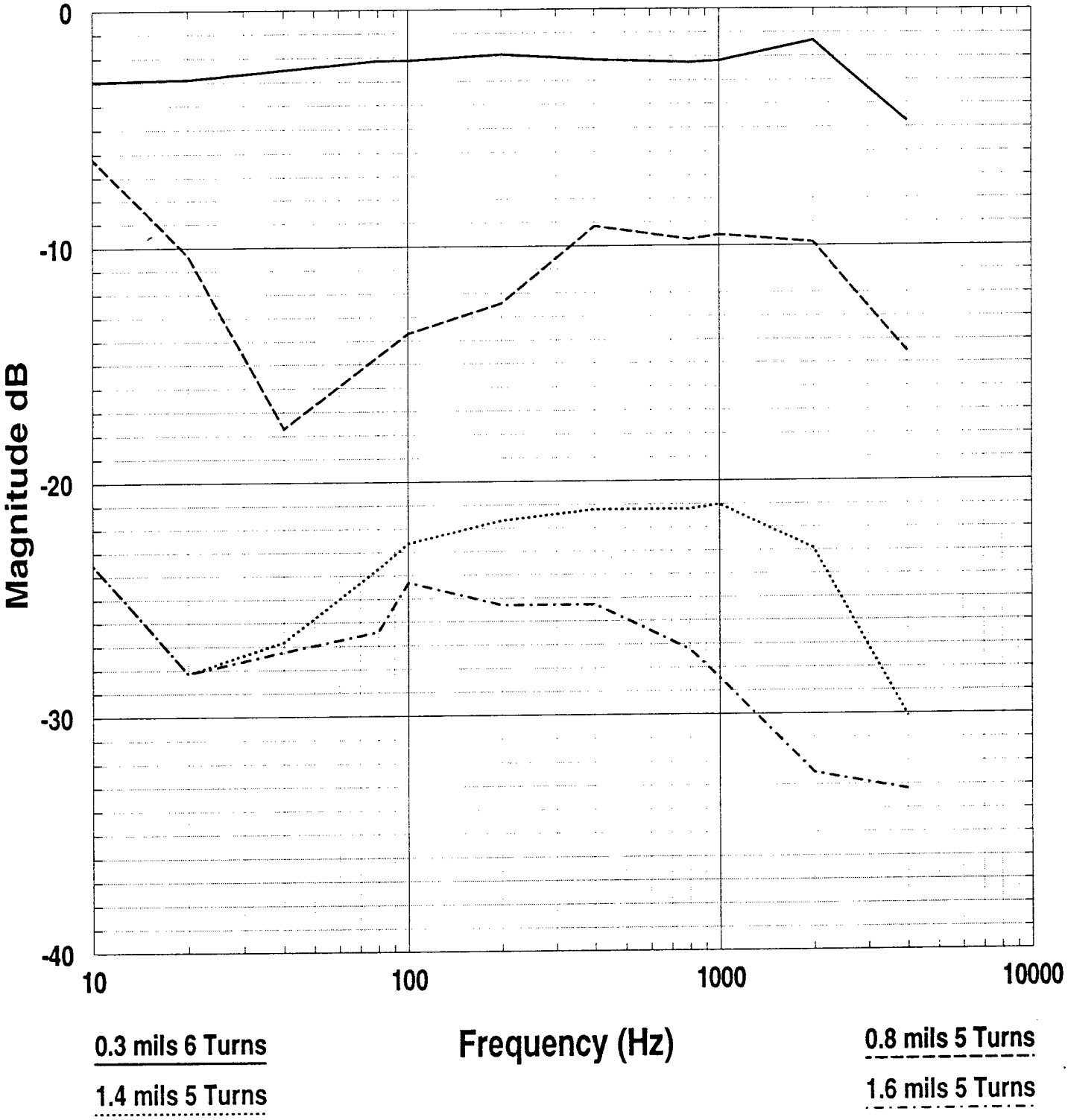

Figure 8. Nickel Alloy Coatings on Copper Foil Wraps

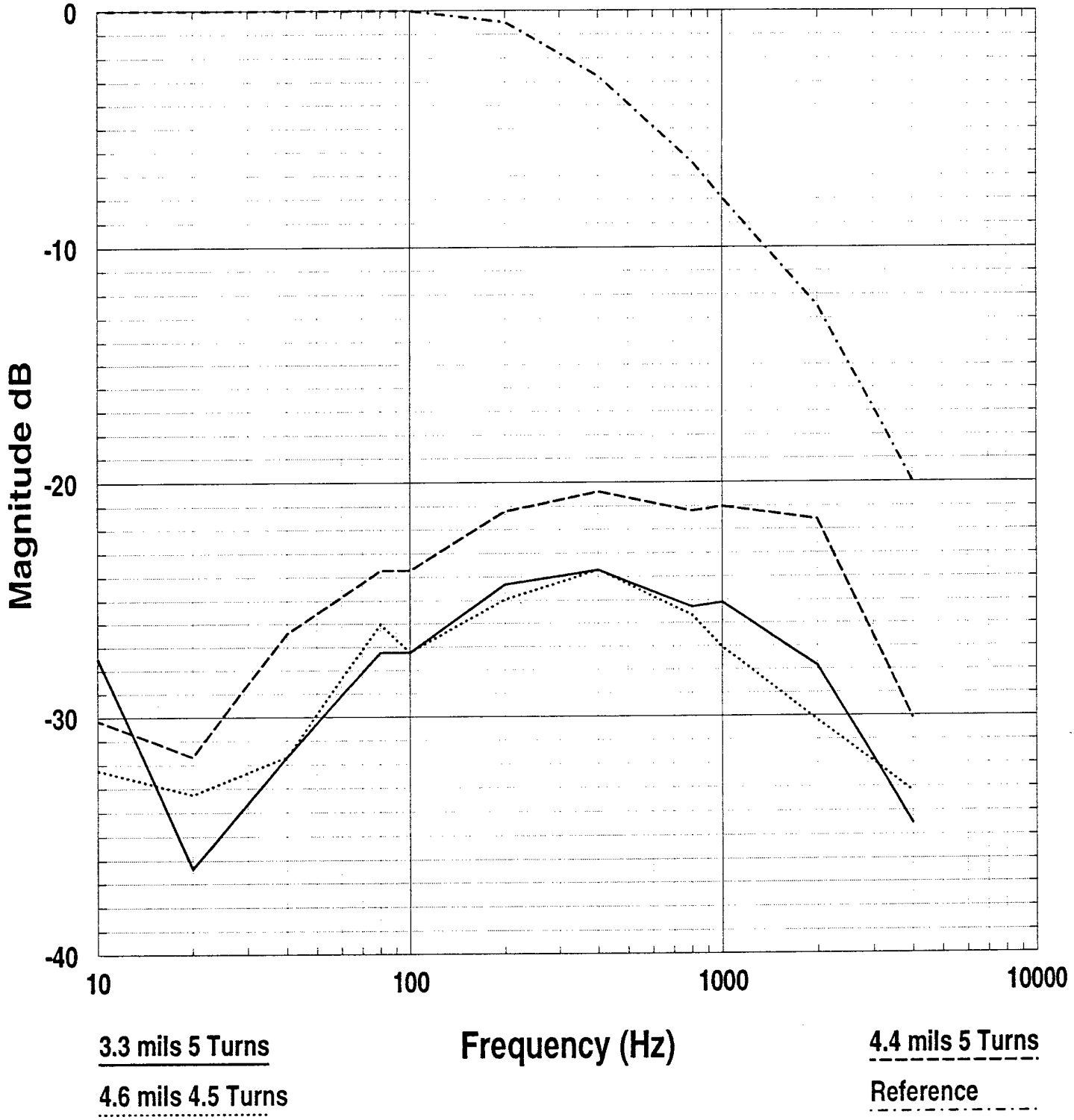

better shielding is obtained with thicker deposits. The trend continues for the data shown in Figure 8, but the results are not as consistent. This may be due to the limit in sensitivity of the instrumentation.

It was observed that the waveform was consistently distorted for frequencies up to 100 or 200 Hz. In general, the distortion was more prevalent in the thinner deposits where saturation is more apt to occur and was causing nonlinear response of the B-field. For runs 5 and 6 the 80 Hz current was reduced by a factor of 20. Under these conditions the distortion disappeared and the shielding appeared to drop by about 12 dB for run 5 and 7 dB for run 6. This indicates that the material is being saturated by the magnetic field strength. Unfortunately the detected signals were very weak and there was not sufficient sensitivity to carry out a systematic study at all frequencies.

There is no evidence that the diameter of the tube has any effect on the transmission coefficient. This is expected since the wavelength of the fields is extremely long compared to any other dimension of the system. As a result, the system can be viewed as one which is in a slowly varying "static field".

Table 6. Comparison of the transmission coefficients (dB) for nickel alloy electrodeposited on copper foil. The thickness is the total thickness of alloy deposited on both sides of the foil.

Freq (Hz)	bare	Run 1	Run 2	Run 3	Run 4	Run 5	Run 6	Run 7
	1.75 turns	5 turns	6 turns	5 turns	5 turns	5 turns	5 turns	4.5 turns
		1.4 mils	0.3 mils	4.4 mils	1.6 mils	3.3 mils	0.8 mils	4.6 mils
		0.8" O.D.	0.9" O.D.	1.0" O.D.	0.8" O.D.	0.9" O.D.	0.9" O.D.	1.1" O.D.
10	0.0	-23.5*	-3.0*	-30.1*	-23.5*	-27.5*	-6.2*	-32.2*
20	0.0	-28.1*	-2.9*	-31.7*	-28.1*	-36.5*	-10.3*	-33.3*
40	0.0	-26.8*	-2.5*	-26.4*	-27.2*	-31.7*	-17.7*	-31.7*
80	0.0	-23.7*	-2.1	-23.7	-26.4	-27.2*	-14.7*	-26.0
100	0.0	-22.6*	-2.1	-23.7	-24.3	-27.2*	-13.7*	-27.2
200	0.0	-21.7	-1.9	-21.2	-25.3	-24.3	-12.4*	-25.0
400	0.0	-21.2	-2.1	-20.4	-25.3	-23.7	-9.2	-23.7
800	-0.3	-21.2	-2.3	-21.2	-27.2	-25.3	-9.7	-25.7
1000	-0.1	-21.0	-2.2	-21.0	-28.5	-25.1	-9.5	-27.0
2000	-0.1	-22.9	-1.3	-21.6	-32.5	-27.9	-9.9	-30.2
4000	-0.6	-30.1	-4.8	-30.1	-33.2	-34.5	-14.5	-33.2

* Indicates that the waveform is distorted.

Table 7 summarizes the averages from Table 6 with the second row showing the average normalized to one turn and one mil thickness. This table shows that the thicker deposits give the better shielding. It is difficult to determine a trend by observing the normalized numbers, although runs 1 and 4 have similar numbers and runs 3 and 7 have similar numbers. Note that the copper foil contributes very little to the average shielding in this frequency range. It contributes less than 0.5 dB for a six turn wrap.

A comparison of Table 7 with Table 5 shows that significant shielding can be obtained by both direct deposit and by wrapping. In general the direct deposit approach

Table 7. Comparison of average transmission coefficient (10 to 4000 Hz) and average transmission coefficient per mil of alloy per turn (estimated copper losses are not included).

bare	Run 1	Run 2	Run 3	Run 4	Run 5	Run 6	Run 7
-0.10	-23.89 dB	-2.47 dB	-24.60 dB	-27.41 dB	-28.26 dB	-11.62 dB	-28.65 dB
	-3.37 dB/mil	-1.18 dB/mil	-1.11 dB/mil	-3.38 dB/mil	-1.71 dB/mil	-2.83 dB/mil	-1.29 dB/mil

appears to use the nickel alloy more effectively. This may be due to the unbroken ring of magnetic material around the direct deposit tube. The wrapping technique might be improved if the layers were brought closer together so that they would appear more like a solid ring of magnetic material.

Measurement Summary

Discussion of Results

Measurements from 10 to 4000 Hz show that magnetic shielding can be obtained from both direct deposition on a tube or by wrapping copper foil with nickel alloy electrodeposited on both sides. The direct deposit offers the most efficient shielding, while the wrapping approach is easier to implement. There is some evidence at the lower frequencies that saturation can occur.

The measurements show that either direct deposit or the wrapping technique can be used to shield. Measurements show that increased alloy deposits increase the shielding. In this study, the thickness of the alloy layer never got great enough to require interleaving the layers with copper layers. The study does show that saturation could be a problem, but there is not enough sensitivity in the pickup probe to quantify saturation effects.

In order to study higher attenuation rates the sensitivity of the detection system must be improved. This could be done by making a new pickup coil which has more turns on it. The total size of the pickup coil is determined by the inside diameter of the smallest gun barrel. The coil could be machine wound to get more turns or a smaller gauge wire could be used. An alternative approach would be to use a broad band voltage amplifier to increase the signal level into the oscilloscope.

CALCULATIONS

Two types of calculations were planned for this study: the first, to use TROMMA to do free space plane wave calculations; the second, to do cylindrical wave calculations.

To do the free space plane wave calculations, Damaskos, Inc.'s proprietary code, TROMMA, was used. This code was run using published values of conductivities for pure copper and for a nickel alloy. The permeability of copper was taken as 1 and a value of 10,000 was used for the nickel alloy. Although the nickel alloy permeability value is half that of the published work, it is closer to the value which has been used in other calculations used to model this material. A summary of the calculations is shown in Table 8. This table shows that the low frequency performance for copper is quite good; this is not in agreement with observations made in the measurements section.

Table 8. Low frequency plane wave transmission coefficients (dB) for three different thicknesses of copper.

	2.5 mils	5 mils	10 mils
10 Hz	-116.8	-122.9	-128.9
100 Hz	-116.8	-122.9	-128.9
1000 Hz	-116.8	-122.9	-128.9
10 000 Hz	-116.8	-122.9	-128.9

Table 9. Low frequency plane wave transmission coefficients (dB) for three different thicknesses of nickel alloy.

	2.5 mils	5 mils	10 mils
10 Hz	-85.6	-91.7	-97.7
100 Hz	-85.6	-91.7	-97.7
1000 Hz	-85.7	-91.9	-100.2
10 000 Hz	-86.8	-100.3	-128.0

Table 9 shows the plane wave transmission coefficient for nickel alloy for the same three thicknesses and frequencies. A comparison of these tables shows the plane wave attenuation of both materials is quite high and that the copper is about 30 dB better at shielding than the alloy. These tables also show that the shielding due to copper is independent of frequency in this frequency range and that the alloy increases its shielding with increasing frequency.

Table 10. Low frequency plane wave transmission coefficients (based on the amount of energy getting into the sample) (dB) for four different thicknesses of copper.

	2.5 mils	5 mils	10 mils	32 mils
10 Hz	-0.00	-0.00	-0.01	-0.03
100 Hz	-0.00	-0.00	-0.01	-0.03
1000 Hz	-0.00	-0.00	-0.01	-0.03
10 000 Hz	-0.00	-0.00	-0.02	-1.92

Table 11. Low frequency plane wave transmission coefficients (based on the amount of energy getting into the sample) (dB) for three different thicknesses of nickel alloy.

	2.5 mils	5 mils	10 mils
10 Hz	-0.00	-0.00	-0.00
100 Hz	-0.00	-0.01	-0.16
1000 Hz	-0.06	-0.94	-8.18
10 000 Hz	-4.44	-18.73	-46.46

Tables 10 and 11 show the planar transmission coefficients for copper and alloy based on the amount of energy entering the metal. Note that the attenuation of the energy is negligible for copper even at the thickest values. The alloy calculations show that it is better at attenuating the energy than the copper. These data show that the lower transmission coefficient of copper in Table 8 is due to the high impedance mismatch for a plane wave at the copper/air interface which means that most of the energy is reflected.

The second approach to calculations was to implement the cylindrical wave model that was outlined in the Phase I proposal. These calculations give similar results as the plane wave calculations at the lower frequencies. At the higher frequencies the results became erratic due to numerical problems in the functions used as solutions. Tables 12 and 13 summarize the results. These calculations show that copper transparency improves with increasing frequency which is not consistent with measured observations. These calculations do show, however, that the nickel alloy is a better low frequency shielding material. Since low frequency results were similar to the plane wave calculations, no further work was conducted using this model and work on a new model was begun.

Table 12. Low frequency cylindrical magnetic wave transmission coefficients (dB) for four different thicknesses of copper.

	2.5 mils	5 mils	10 mils	32 mils
10 Hz	-100.63	-106.67	-112.75	-123.09
100 Hz	-91.69	-97.73	-103.81	-114.15
1000 Hz	-82.90	-88.94	-95.01	-105.35
10 000 Hz	-77.37	-65.31	-71.39	-82.13

Table 13. Low frequency plane wave transmission coefficients (dB) for three different thicknesses of nickel alloy.

	2.5 mils	5 mils	10 mils
10 Hz	-124.94	-130.97	-137.05
100 Hz	NAN	NAN	NAN
1000 Hz	NAN	NAN	NAN
10 000 Hz	NAN	NAN	NAN

NAN = Not a number.

The new model, which focused on just the magnetic field, is given in Appendix B. This is a single layer model and the results are summarized in Tables 14, 15 and 16. As these data show, numerical problems are present in this formulation as well. The results in

Table 14, for example, that are erratic or inconsistent are so noted based purely on a subjective appraisal. The remaining entries suggest that copper shielding of magnetic field is proportional to the square of thickness and increases rapidly with frequency, following the behavior of the copper reference of Figure 4. The data of these tables generally do show trends that are supported by measurements. These observations are that copper

Table 14. Low frequency cylindrical magnetic wave transmission coefficients (dB) for four different thicknesses of copper.

	2.5 mils	5 mils	10 mils	32 mils
10 Hz	-0.00 erratic	-0.14 erratic	-0.47 erratic	-2.76
100 Hz	8.81 erratic	6.68 erratic	2.73 erratic	-6.87
1000 Hz	6.94 erratic	1.15 erratic	-4.85	-15.48
10 000 Hz	-1.31	-7.34	-13.42	-24.56

Table 15. Low frequency plane wave transmission coefficients (dB) for three different thicknesses of mu =10000.

	2.5 mils	5 mils	10 mils
10 Hz	-55.54	-55.60	-55.73
100 Hz	-INF	-INF	-INF
1000 Hz	-INF	-INF	-INF
10 000 Hz	-INF	-INF	-INF

Table 16. Low frequency plane wave transmission coefficients (dB) for three different thicknesses of mu = 2500.

	2.5 mils	5 mils	10 mils
10 Hz	-49.52	-49.58	-49.70
100 Hz	-39.53	-39.61	-39.81
1000 Hz	-INF	-INF	-INF
10 000 Hz	-INF	-INF	-INF

provides very little shielding at low frequencies, even at 32 mil thickness, while thin layers of nickel alloy give good shielding.

As a final calculation, the transmission coefficients for several thicknesses of copper and nickel alloy were computed using the attenuation based on skin depth (8.686 t/δ dB). This simple calculation shows the transparency of the copper and it shows that the nickel alloy gives better shielding, but neither of the alloy results are in agreement with the measurements at the lowest frequencies. No further work was done on calculations since the additional effort required is beyond the scope of the Phase I project.

Table 17. Transmission coefficients (dB) for four different thicknesses of copper computed based on the skin depth penetration.

	2.5 mils	5 mils	10 mils	32 mils
10 Hz	-0.03	-0.05	-0.11	-0.34
100 Hz	-0.08	-0.17	-0.33	-1.07
1000 Hz	-0.26	-0.53	-1.06	-3.38
10 000 Hz	-0.83	-1.67	-3.34	-10.68

Table 18. Low frequency plane wave transmission coefficients (dB) for three different thicknesses of mu = 10000 computed based on the skin depth penetration.

	2.5 mils	5 mils	10 mils
10 Hz	-0.44	-0.88	-1.75
100 Hz	-1.39	-2.77	-5.54
1000 Hz	-4.38	-8.77	-17.53
10 000 Hz	-13.86	-27.72	-55.45

Table 19. Low frequency plane wave transmission coefficients (dB) for three different thicknesses of mu = 5000 computed based on the skin depth penetration.

	2.5 mils	5 mils	10 mils
10 Hz	-0.31	-0.62	-1.24
100 Hz	-0.98	-1.96	-3.92
1000 Hz	-3.10	-6.20	-12.40
10 000 Hz	-9.80	-19.60	-39.21

Calculations Summary

The free space plane wave calculations are inadequate to describe the low frequency performance of the copper and nickel alloy materials. And, the best model appears to be one that focuses only on the magnetic field. At this time it appears as though the major limitation is in the formulation, which encounters numerical difficulties as the complex arguments get large or too small.

CONCLUSIONS AND RECOMMENDATIONS

The feasibility of using ThinShield™ materials to provide significant low frequency attenuation of magnetic fields in a cylindrical coordinate geometry of high aspect ratio (length to diameter) is established. Magnetic shielding effectiveness of the order of 30 dB in the broad 10 to 1000 Hz band are feasible when geometric control can be imposed. The rough order of a ThinShield™ material layer pair is 10 mils of nickel alloy over a copper base. The base is believed to be much thinner than the 33 mil tube used as the scaled gun barrel. The average magnetic shielding effectiveness is $\approx$2.2 dB/mil of direct deposit alloy.

Non-magnetic material shielding at these frequencies, e.g. copper alone, is not effective below about 1000 Hz where the skin depth of 82 mils is 2.5 times the 32 mil copper tube thickness. At 200 Hz the measured effectiveness is only $\approx$1 dB increasing monotonically with frequency to 8 dB at 1000 Hz. But the addition of only 3.9 mils of magnetic material to form a one layer pair ThinShield™ coating increases the shielding effectiveness by 15 dB across the measured band from 10 to 3000 Hz and an 11 mil magnetic coating, by about 25 dB. Despite the various difficulties in the experimental setup described earlier, the improvement is notable, significant and consistent with the project goal of attaining 30 dB of shielding.

The single layer cylindrical tube analysis and computational tool could only give a qualitative confirmation of the copper film shielding effectiveness with frequency. Numerical difficulties in the computation of a single layer of magnetic material could not be resolved and when such computations could be performed the results appeared counter to intuition. The original cylindrical tube multilayer formulation that was proposed for design guidance suffered numerical difficulties that prevented meaningful calculations. The large complex arithmetic arguments of the Hankel functions caused overflows during the computations. The analyses also require differences in very like quantities where high precision (64 bits was employed) is required and a numerically significant difference is difficult to attain. The originally proposed model is a high impedance (E-field) model whereas the newer formulation is a low impedance (H-field) model and is more suitable. With a second layer, the model is a predictive tool for direct deposition and would be considered in a later phase of the program.

Multiple wraps around the scaled gun copper tube were made. The wrap, a three layer ThinShield™, with copper foil in the center, could circumscribe the tube up to 6 times. The shielding increment again was significant, typically of the order of 25 dB with only about 1.5 mils of total alloy thickness but control over this part of the work is not as close as for direct deposition. The average magnetic shielding effectiveness of the 1.5 mils total alloy thickness ThinShield™ wrap is $\approx$3.4 dB/mil. Effects of the gap and tradeoffs of layer thickness and number of wraps could not be thoroughly quantified during Phase I.

Important experience was obtained in the preparation of plating baths and setups for the direct deposition and for the planar sheet ThinShield™ coatings. This know how will aid the scale up of the processes to a larger size for realistic and possibly actual demonstrations of rail gun shielding during a Phase II effort.

In like vane, the measurement techniques experience of Phase I highlights shortcomings and limitations in setup that must be improved for follow-on work to proceed. Measurements that are accurate and sensitive are important to the ThinShield™ materials design process in this shielding application.

Lastly, both key applications, rail gun shielding and power buss shielding, are shown to be feasible in the 10 to 1000 Hz band and, by inference and prior experience, above the band using Damaskos, Inc.'s ThinShield™ materials.

Recommendations

In a follow-on Phase II effort that would pursue meaningful applications of this low frequency magnetic shielding work, these recommendations would be pursued in conjunction with feed back and input from the Army sponsors.

1. First is to determine the requirements for a demonstration on the next larger scale of rail gun shielding; then scale up the process accordingly. Some input would be available from a Phase II proposal. This activity would involve coordination with the Army and others.

2. Improve both the magnetic field generating setup and the sensitivity for detection of weak fields. It is desirable to be able to measure shielding effectiveness in the linear portion of the shielding materials' B-H curve in order to be able to be guided by

comparable (linear) magnetic field analysis.

3. Develop a cylindrical coordinate model with magnetic field excitation that will permit a multilayered coating structure to be analyzed and use the model to design the coating and predict performance.

4. Quantify the effects of breaks in the continuity of a wrappable shielding coating and develop a joining technique to minimize the loss in shielding performance of the coating. Consider the import of caps that are designed as shielding enclosures for parts and so serve as adjuncts to the tubular shields.

5. Identify other practical issues and propose solutions.

6. Estimate the cost of applying the shielding to actual structures.

7. Propose and assist in the design of a field test demonstration at the larger scale level. Work with Army personnel to define a meaningful scale up demonstration.

8. Seek out improved technique for making the ThinShield™ materials in wrappable form of sufficient width and length to be able to execute the next level scale up.

9. Propose other applications of this technology.

10. Develop further the direct deposition ThinShield™ "tubes" to the point where they may be used as conduit for shielding magnetic fields in "critical" power generation applications. An important aspect of this activity is to determine the loss of shielding efficiency at the breaks (ends) of the tubular section of the shield and to find a way to reduce or eliminate such loss of shielding efficiency.

11. Generally explore applications that will enhance safety and health such as selected shielding in hospital applications, shielding home everyday products such as high current hair dryers, improved shielding wires for use in electric blankets, and others.

REFERENCES

[1] Metals Handbook 9th edition; Volume 5, American Society for Metals, 1988; Metals Park, Ohio 44073, pp. 199-207.

[2] "TROMMA: Multilayer planewave geometry code for anisotropic materials," Damaskos, Inc. proprietary code.

APPENDIX A - CYLINDRICAL WAVE ELECTRIC FIELD SHIELDING ANALYSIS

To model the effectiveness of a Thin-Shield™ coating material for the electric gun application the following analysis, presented in outline form. Figure A-1 depicts the geometry of the problem in which a current line source is shielded by a multilayer mixed composite.

This is a classical boundary value problem which consists of finding the axial electric fields E_z and the circumferential fields H_ϕ. For $\rho \geq b$

$$E_z = E_b \frac{H_o^{(2)}(k_o \rho)}{H_o^{(2)}(k_o b)} \; ; \quad k_o = \omega \sqrt{\mu_o \epsilon_o}$$

$$H_\phi = -\frac{E_b}{j \eta_o} \frac{H_1^{(2)}(k_o \rho)}{H_0^{(2)}(k_o b)} \; ; \quad \eta_o = \sqrt{\frac{\mu_o}{\epsilon_o}} = 120 \; \pi \Omega.$$

$$E_b = E_a \prod_{n=1}^{N} \frac{N_o(s_n) - X_n J_o(s_n)}{N_o(t_n) - X_n J_o(t_n)}$$

for

$$t_n = k_n \rho_{n-1}$$

$$s_n = k_n \rho_n$$

$$k_n = k_o \sqrt{\mu_{nr} \epsilon_{nr}}$$

$$\eta_n = \eta_o \sqrt{\mu_{nr} / \epsilon_{nr}}$$

"r" denotes relative to free space

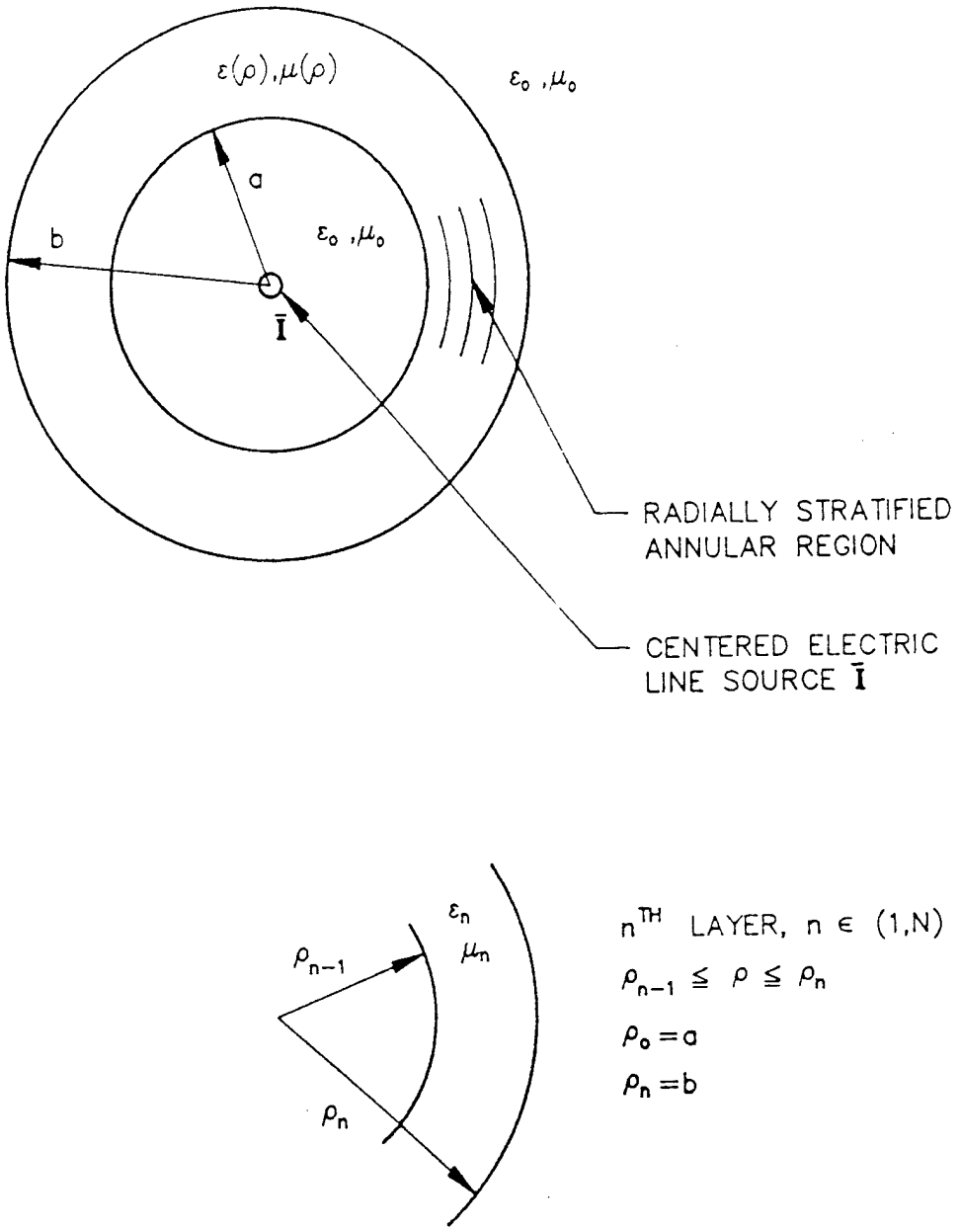

Figure A-1. Cylindrical geometry with no ϕ dependence for shielding of a line source.

$$X_n = \frac{N_o(s_n) + \zeta_n N_1(s_n)}{J_o(s_n) + \zeta_n J_1(s_n)}$$

where the ζ_n's are to be calculated from the downwards relationship:

$$\frac{\eta_{n-1}}{\eta_n}\,\zeta_{n-1} = \frac{[N_o(s_n)J_o(t_n) - N_o(t_n)J_o(s_n)] + \zeta_n[N_1(s_n)J_o(t_n) - N_o(t_n)J_1 s_n)]}{[N_1(t_n)J_o(s_n) - J_1(t_n)N_o(s_n)] + \zeta_n[N_1(t_n)J_1(s_n) - J_1(t_n)N_1(s_n)]}$$

for $n \in (1,N)$, which is started from $n=N$:

$$\zeta_N = -H_o^{(2)}(k_o b)/H_1^{(2)}(k_o b)$$

and concludes with the calculation of ζ_o. Finally:

$$E_a = -\frac{\eta_o k_o}{4} I \left\{H_o^{(2)}(k_o a) + \gamma J_o(k_o a)\right\}$$

$$\gamma = -\frac{J_o(k_o a) + \zeta_o J_1(k_o a)}{H_o^{(2)}(k_o a) + \zeta_o H_1^{(2)}(k_o a)}.$$

The above relations are all the equations necessary to calculate the transmitted field for $\rho \geq b$.

The measure of cylindrical wave electric field shielding efficiency is obtained by dividing the above fields E_z and H_ϕ by the fields in the absence of the shield for $\rho \geq b$:

$$E_{z_o} = -\frac{\eta_o k_o}{4} I\, H_o^{(2)}(k_o \rho)$$

$$H_{\phi_o} = \frac{k_o I}{4j}\, H_1^{(2)}(k_o \rho).$$

APPENDIX B - CYLINDRICAL WAVE MAGNETIC FIELD SHIELDING ANALYSIS

This low frequency analysis is for a single layer coating of material that surrounds a source of magnetic field and is characterized by its bulk conductivity σ, permeability relative to free space μ, and relative dielectric constant ϵ. The geometry is illustrated in this sketch. Both the electric and magnetic field intensities at the inner boundary of the coating are not required to specify the problem adequately. Since we are interested only in the low impedance wave magnetic field shielding efficiency, we choose the magnetic field intensity as the inner boundary condition. This is a low frequency magnetostatic assumption and can be related via ampere's law to an interior axial current I_z amperes, whose azimuthal magnetic field intensity is H_ϕ amperes per meter; i.e. $H_\phi(a-) = I_z/2\pi a = B/\eta_o$. Then the boundary conditions at both, inner and outer surfaces of the coating require that the magnetic and electric fields be continuous and can be written as follows:

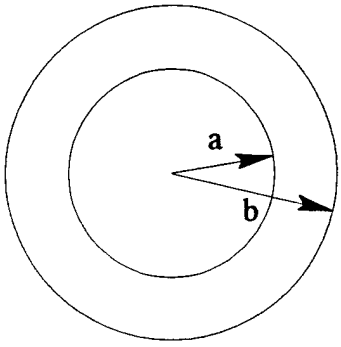

$$@r=a \quad \frac{B}{\eta_o} H_1^{(2)}(k_o a) = \frac{A_1}{\eta} H_1^{(1)}(ka) + \frac{B_1}{\eta} H_1^{(2)}(ka)$$

$$@r=b \quad \frac{A_1}{\eta} H_1^{(1)}(kb) + \frac{B_1}{\eta} H_1^{(2)}(kb) = \frac{B_2}{\eta_o} H_1^{(2)}(k_o b)$$

$$A_1 H_o^{(1)}(kb) + B_1 H_o^{(2)}(kb) = B_2 H_o^{(2)}(k_o b)\,.$$

In these equations $H_o^{(2)}$ and $H_1^{(2)}$ are radially outward propagating cylindrical waves and $H_o^{(1)}$ and $H_1^{(1)}$ propagate inward. Upon eliminating A_1 and B_1 from these relationships we obtain the ratio of the magnetic fields at the outer and inner boundaries which defines the magnetic shielding; i.e.

$$\begin{matrix} \textit{magnetic shielding} \\ \textit{efficiency} \end{matrix} = |B_2/B|^2$$

where,

$$\frac{B_2}{B_1} = \frac{2/(\pi kb)}{\frac{\eta}{\eta_o} H_1^{(2)}(k_o b)\left[Y_o(kb)J_1(ka) - J_o(kb)Y_1(ka)\right] - H_o^{(2)}(k_o b)\left[Y_1(kb)J_1(ka) - J_1(kb)Y_1(ka)\right]}$$

and

$$k = k_o\sqrt{\mu_r\epsilon_r} = \frac{2\pi}{\lambda_o}\sqrt{\mu_r\epsilon_r}$$

$$\frac{\eta}{\eta_o} = \sqrt{\frac{\mu_r}{\epsilon_r}}$$

$$\epsilon_r = |\epsilon_r'|\left(1 - j\frac{\sigma}{\omega_o\epsilon_o}\right) = \epsilon' - j\epsilon''$$

$$\mu_r = |\mu_r'|\,(1 - j\tan\delta_m) = \mu' - j\mu''$$

$$H_o^{(1)} = J_o + jY_o$$

$$H_o^{(2)} = J_o - jY_o$$

$$H_1^{(1)} = J_1 + jY_1$$

$$H_1^{(2)} = J_1 - jY_1$$

a = *inner radius of coating*

b = *outer radius of coating*.